Supplementary Information

# A mechanistic link between cellular trade-offs, gene expression and growth

Andrea Y. Weiße, Diego A. Oyarzún, Vincent Danos, Peter S. Swain

## Contents

# S1 Model definition

## S1.1 Overview

We consider a mechanistic model of the cell. It combines nutrient import and its conversion to cellular energy with the biosynthetic processes of transcription and translation. In its basic form, the model includes 14 intracellular variables: internal nutrient $s_i$; energy, $a$, such as ATP[1]; and four types of proteins along with their corresponding free and ribosome-bound mRNAs. The four types of proteins we consider are (1) ribosomes $r$, (2) a transporter enzyme $e_t$ and (3) a metabolic enzyme $e_m$, and (4) a class of house-keeping proteins $q$. We denote the corresponding free mRNAs by $m_x$ and ribosome-bound mRNA by $c_x$ with $x \in \{r, t, m, q\}$.

Table S1: List of reactions considered.

| | dilution | transcription | dilution/degradation | ribosome binding | dilution | translation |
|---|---|---|---|---|---|---|
| ribosomes | $r \xrightarrow{\lambda} \varnothing$ | $\varnothing \xrightarrow{\omega_r} m_r$ | $m_r \xrightarrow{\lambda+d_m} \varnothing$ | $r + m_r \underset{k_u}{\overset{k_b}{\leftrightarrow}} c_r$ | $c_r \xrightarrow{\lambda} \varnothing$ | $n_r\, a + c_r \xrightarrow{\nu_r} r + m_r + r$ |
| transporter enzyme | $e_t \xrightarrow{\lambda} \varnothing$ | $\varnothing \xrightarrow{\omega_t} m_t$ | $m_t \xrightarrow{\lambda+d_m} \varnothing$ | $r + m_t \underset{k_u}{\overset{k_b}{\leftrightarrow}} c_t$ | $c_t \xrightarrow{\lambda} \varnothing$ | $n_t\, a + c_t \xrightarrow{\nu_t} r + m_t + e_t$ |
| metabolic enzyme | $e_m \xrightarrow{\lambda} \varnothing$ | $\varnothing \xrightarrow{\omega_m} m_m$ | $m_m \xrightarrow{\lambda+d_m} \varnothing$ | $r + m_m \underset{k_u}{\overset{k_b}{\leftrightarrow}} c_m$ | $c_m \xrightarrow{\lambda} \varnothing$ | $n_m\, a + c_m \xrightarrow{\nu_m} r + m_m + e_m$ |
| growth-independent proteins | $q \xrightarrow{\lambda} \varnothing$ | $\varnothing \xrightarrow{\omega_q} m_q$ | $m_q \xrightarrow{\lambda+d_m} \varnothing$ | $r + m_q \underset{k_u}{\overset{k_b}{\leftrightarrow}} c_q$ | $c_q \xrightarrow{\lambda} \varnothing$ | $n_q\, a + c_q \xrightarrow{\nu_q} r + m_q + q$ |
| internal nutrient | $s_i \xrightarrow{\lambda} \varnothing$ | $s \xrightarrow{\nu_{\text{imp}}} s_i$ | $s_i \xrightarrow{\nu_{\text{cat}}} n_s\, a$ | | | |
| ATP | $a \xrightarrow{\lambda} \varnothing$ | nutrient import | metabolism | | | |

We model the cell as a system of ordinary differential equations derived from the

[1]Similarly $a$ can also be interpreted as amino acids, or any other essential resource for biosynthetic reactions.

reactions listed in Table S1:

$$\dot{s}_i = \nu_{\text{imp}}(e_t, s) - \nu_{\text{cat}}(e_m, s_i) - \lambda \cdot s_i, \tag{1}$$

$$\dot{a} = n_s \cdot \nu_{\text{cat}}(e_m, s_i) - \sum_{\substack{x \in \\ \{r,t,m,q\}}} n_x \cdot \nu_x(c_x, a) - \lambda \cdot a, \tag{2}$$

$$\dot{r} = \nu_r(c_r, a) - \lambda \cdot r + \sum_{\substack{x \in \\ \{r,t,m,q\}}} (\nu_x(c_x, a) - k_b \cdot r \cdot m_x + k_u \cdot c_x), \tag{3}$$

$$\begin{aligned} \dot{e}_t &= \nu_t(c_t, a) - \lambda \cdot e_t, \\ \dot{e}_m &= \nu_m(c_m, a) - \lambda \cdot e_m, \\ \dot{q} &= \nu_q(c_q, a) - \lambda \cdot q, \end{aligned} \tag{4}$$

$$\dot{m}_x = \omega_x(a) - (\lambda + d_m) \cdot m_x + \nu_x(c_x, a) - k_b \cdot r \cdot m_x + k_u \cdot c_x, \tag{5}$$

$$\dot{c}_x = -\lambda \cdot c_x + k_b \cdot r \cdot m_x - k_u \cdot c_x - \nu_x(c_x, a), \qquad x \in \{r, t, m, q\}\,. \tag{6}$$

We consider all variables in molecules per cell. The units of the parameters and their default values are listed in Table S2. The growth rate $\lambda = \lambda(\sum_x c_x, a)$ is a function of the number of translating ribosomes and energy, and $q$-transcription, in Eq. (5) when $x = q$, is a function $\omega_q(q, a)$ of the level of $q$-protein and energy. Below we elaborate on the main assumptions of the model and on the derivation of the kinetic reaction rates.

## S1.2 Derivation of reaction rates

### S1.2.1 Main assumptions

Apart from the three main trade-offs elaborated in the main text (finite energy, finite ribosomes and finite proteome) we base our model on the following assumption:

1. First-order dilution of the intracellular species;
2. No degradation of proteins (although it can be included) and first-order degradation of mRNA;
3. Mass action kinetics for the binding and unbinding of mRNAs with free ribosomes;
4. Energy consumption within the cell is from translation and we neglect the consumption from transcription [17, 21].

### S1.2.2 Nutrient import and metabolism

We assume the enzymatically catalyzed reactions, nutrient import and metabolism, to be saturable and use Michaelis-Menten kinetics with maximal rates $v_t$ and $v_m$ and

Table S2: Model parameters. Default values were used unless otherwise stated. ★Obtained by parameter optimization (see §S3 for details). †Chosen relative to $K_t$; ‡such that maximal growth rate matches that of *E. coli*; §*E. coli* average; ♯for steep auto-inhibition; *near diffusion limit; ◇order of magnitude; aa denotes number of amino acids.

| | description | default value | unit | source |
|---|---|---|---|---|
| $s$ | external nutrient | $10^4$ | [molecs] | † |
| $d_m$ | mRNA-degradation rate | 0.1 | $[\text{min}^{-1}]$ | [20] |
| $n_s$ | nutrient efficiency | 0.5 | none | ‡ |
| $n_r$ | ribosome length | 7459 | $[^{\text{aa}}/_{\text{molecs}}]$ | [12] |
| $n_x$, $x \in \{t, m, q\}$ | length of non-ribosomal proteins | 300 | $[^{\text{aa}}/_{\text{molecs}}]$ | [2]§ |
| $\gamma_{\max}$ | max. transl. elongation rate | 1260 | $[^{\text{aa}}/_{\text{min molecs}}]$ | [3] |
| $K_\gamma$ | transl. elongation threshold | 7 | $[^{\text{molecs}}/_{\text{cell}}]$ | ★ |
| $v_t$ | max. nutrient import rate | 726 | $[\text{min}^{-1}]$ | [7] |
| $K_t$ | nutrient import threshold | 1000 | [molecs] | |
| $v_m$ | max. enzymatic rate | 5800 | $[\text{min}^{-1}]$ | [1] |
| $K_m$ | enzymatic threshold | 1000 | $[^{\text{molecs}}/_{\text{cell}}]$ | |
| $w_r$ | max. ribosome transcription rate | 930 | $[^{\text{molecs}}/_{\text{min cell}}]$ | ★ |
| $w_e = w_t = w_m$ | max. enzyme transcription rate | 4.14 | $[^{\text{molecs}}/_{\text{min cell}}]$ | ★ |
| $w_q$ | max. $q$-transcription rate | 948.93 | $[^{\text{molecs}}/_{\text{min cell}}]$ | ★ |
| $\theta_r$ | ribosome transcription threshold | 426.87 | $[^{\text{molecs}}/_{\text{cell}}]$ | ★ |
| $\theta_{\text{nr}}$ | non-ribosomal transcription threshold | 4.38 | $[^{\text{molecs}}/_{\text{cell}}]$ | ★ |
| $K_q$ | $q$-autoinhibition threshold | 152 219 | $[^{\text{molecs}}/_{\text{cell}}]$ | ★ |
| $n_q$ | $q$-autoinhibition Hill coeff. | 4 | none | ♯ |
| $k_b$ | mRNA-ribosome binding rate | 1 | $[^{\text{cell}}/_{\text{min molecs}}]$ | * |
| $k_u$ | mRNA-ribosome unbinding rate | 1 | $[\text{min}^{-1}]$ | |
| $M$ | total cell mass | $10^8$ | [aa] | [3]◇ |
| $k_{\text{cm}}$ | chloramphenicol-binding rate | 0.00599 | $[(\text{min}\,\mu M)^{-1}]$ | ★ |

half-maximal thresholds $K_t$ and $K_m$, such that

$$\nu_{\text{imp}}(e_t, s) = e_t \frac{v_t \cdot s}{K_t + s}, \qquad \nu_{\text{cat}}(e_m, s_i) = e_m \frac{v_m \cdot s_i}{K_m + s_i}. \tag{7}$$

In the basic cell model, we consider a constant environment, and so the external nutrient $s$ is a constant parameter. In §S6 we show how to extend the basic model to include a dynamic environment. The nutrient efficiency parameter, $n_s$, determines energy yield per molecule of $s_i$.

#### S1.2.3 Translation

In exponentially growing microbes, protein synthesis, in particular translation-associated processes, accounts for a major part of the energy budget [17, 21, 22]. Here we assume a simplified mechanism, illustrated in Fig. S1, to derive the dependence of the translation rates on the energy levels of the cell. Using the rate constants in Fig. S1 and

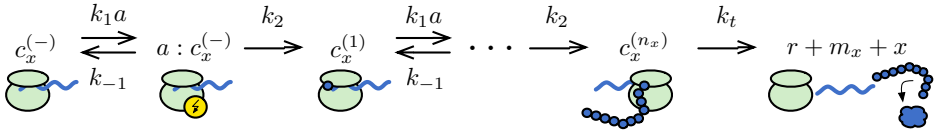


Figure S1: A simplified mechanism of translation. In a reversible reaction, the mRNA-ribosome complex, $c_x$, binds energy. In a second step, the nascent peptide chain elongates by one amino acid consuming energy. The two steps are repeated $n_x$ times, where $n_x$ is the length in amino acids of protein $x$. Finally, termination of translation releases the ribosome, the mRNA and the newly synthesised protein.

defining $K_p := \frac{k_1 k_2}{k_{-1}+k_2}$, we can derive the net rate [5] of translating a protein $x$ as

$$\nu_x(c_x, a) = c_x \cdot \left( n_x \cdot \left( \frac{1}{K_p a} + \frac{1}{k_2} \right) + \frac{1}{k_t} \right)^{-1}. \tag{8}$$

Assuming that the final termination step is fast, $\frac{1}{k_t} \ll n_x \left( \frac{1}{K_p a} + \frac{1}{k_2} \right)$, we write $\nu_x$ as

$$\nu_x(c_x, a) \approx c_x \cdot \frac{\gamma(a)}{n_x}, \qquad \gamma(a) := \frac{\gamma_{\max} a}{K_\gamma + a}, \tag{9}$$

where $n_x$ is the length of protein $x$ (in amino acids) and $\gamma$ is the rate of translational elongation with maximal rate $\gamma_{\max} = k_2$ and threshold $K_\gamma = {}^{k_2}/_{K_p}$ for half-maximal elongation.

#### S1.2.4 Transcription

The contribution of transcription-associated processes to the overall consumption of energy is small compared to that of translation (less than 10% in rapidly growing *E. coli* and *S. cerevisiae* [17, 21]), and so we neglect this contribution to energy consumption.

We do, however, let transcription be an energy-dependent process that ceases when the cell runs out of energy. Analogous to translation (see Fig. S1), transcription involves repeated steps of elongation that each depend on energy. If we assume that the energy consumed in each elongation step is constant, it follows that the effective transcription rate has the form

$$\omega_x(a) = w_x \cdot \frac{a}{\theta_x + a}, \qquad x \in \{r, t, m\}. \tag{10}$$

Unlike the translational elongation thresholds, the transcriptional thresholds $\theta_x$ depend on the gene $x$. We distinguish two transcriptional thresholds, $\theta_x = \theta_{\text{nr}}$ for all non-ribosomal genes $x \in \{t, m, q\}$ and $\theta_r \neq \theta_{\text{nr}}$, because ribosomal expression may have a different sensitivity to physiological changes within the cell. The maximal rate of transcription, $w_x$, is a lumped description of the speed of transcriptional elongation, on the one hand, and gene-related information such as copy number, induction and length, on the other. We assume that the transporter and the metabolic enzymes, $e_t$ and $e_m$, are co-regulated and so $w_t = w_m = w_e$.

We further assume that all but the $q$-proteins have a transcription rate that solely depends on energy levels. The $q$-proteins, we assume, are auto-regulated to sustain stable protein levels across different growth conditions. Following [14], we thus model the effective rate of $q$-transcription by

$$\omega_q(q, a) = w_q \cdot \frac{a}{\theta_x + a} \cdot \mathcal{I}(q), \quad \text{with} \quad \mathcal{I}(q) := \frac{1}{1 + (q/K_q)^{n_q}}, \tag{11}$$

where $\mathcal{I}$ is the auto-inhibition function with threshold $K_q$ and Hill-coefficient $n_q$.

#### S1.2.5 Growth and dilution

Crucial to connecting the cellular processes with growth is the growth rate $\lambda$, which dilutes all intracellular species because of the redistribution of the cellular content to the mother and daughter cell (Table S1). Define the total mass of the cell to be

$$M = \sum_x n_x x + n_r \sum_x c_x \tag{12}$$

and the number of translating ribosomes $\sum_x c_x$ to be $R_t$, we can show that

$$\frac{dM}{dt} = \gamma(a) R_t - \lambda M. \tag{13}$$

At steady-state, the growth rate

$$\lambda = \frac{\gamma(a) R_t}{M} \tag{14}$$

is therefore proportional to the rate of protein synthesis, which agrees with definitions of growth rate elsewhere [8, 18, 19].

We emphasize that specifying a value for $M$, the typical mass of proteins in the cell (in numbers of amino acids), is necessary to fully parameterize our model and by doing so we impose the constraint Eq. 12, and so the trade-off in levels of proteins, when $\lambda$ obeys Eq. 14. We assume that Eq. (14) also holds away from steady-state.

## S2 Bacterial growth laws

The phenomena recently termed 'bacterial growth laws' are empirical relations between the growth rate and the ribosomal mass fraction of exponentially growing cells [19] and Monod's law, which states a Michaelis-Menten-type relation between growth rate and extracellular nutrient [16]. Previous work used phenomenological models to explain the growth laws [18, 13]. Here we derive the bacterial growth laws from our mechanistic model.

### S2.1 The first law

The total amount of ribosomes obeys

$$R = r + R_t \tag{15}$$

with $r$ being the amount of free ribosomes. From the definition of growth rate, Eq. (14), we can therefore write at steady-state [18]:

$$\lambda = \frac{1}{\tau_\gamma}\left(\phi_R - \phi_r\right), \tag{16}$$

with the mass fractions $\phi_R = n_r R/M$ and $\phi_r = n_r r/M$, and $\tau_\gamma = {}^{n_r}/_{\gamma}$ denotes the ribosome synthesis time, that is, the time it takes to translate one ribosome and is a measure of ribosome efficiency. Eq. (16) is the first growth law if $\tau_\gamma$ is approximately constant for changes in extracellular nutrient.

### S2.2 The second law

#### S2.2.1 Balancing energy fluxes

Consider the equation for cellular energy

$$\frac{da}{dt} = n_s e_m \frac{v_m s_i}{K_m + s_i} - \gamma R_t - \lambda a. \tag{17}$$

Then, at steady-state,

$$\lambda \frac{a}{M} + \lambda = \frac{\phi_m}{n_m}\frac{v_m s_i}{K_m + s_i}, \tag{18}$$

using Eq. (14) and dividing through by $M$, where $\phi_m = n_m e_m/M$. We define the metabolic synthesis time $\tau_m = {}^{n_m}/_{n_s v_m}$, the minimal time taken by an enzyme to generate sufficient energy to synthesize another metabolic enzyme, as a measure of metabolic efficiency. Assuming $a \ll M$ at steady-state, then Eq. (18) becomes

$$\lambda \simeq \frac{\phi_m}{\tau_m}\frac{s_i}{K_m + s_i}, \tag{19}$$

and relates growth rate to the mass fraction of a 'bottleneck' metabolic enzyme, $\phi_m$ [18].

We can also consider the total amount of energy either free or bound up in proteins. We find that

$$\frac{d}{dt}(M + n_s s_i + a) = n_s \nu_{\text{imp}} - \lambda(M + n_s s_i + a) \tag{20}$$

and so, at steady-state,

$$\frac{\phi_t}{n_t} \frac{n_s v_t s}{K_t + s} = \lambda \left(1 + n_s \frac{s_i}{M} + \frac{a}{M}\right), \tag{21}$$

writing the transporter mass fraction as $\phi_t = n_t e_t / M$. Eq. (21) shows that the total influx of energy matches the total efflux of energy at steady-state. Analogous to the metabolic synthesis time $\tau_m$, we define the transporter synthesis time $\tau_t = {}^{n_t}/_{n_s v_t}$ to denote the minimal time taken by a transporter to import sufficient nutrient to make another transporter as a measure of the efficiency of transport. If $s_i \ll M$ and $a \ll M$ at steady-state, then Eq. (21) becomes

$$\frac{\phi_t}{\tau_t} \frac{s}{K_t + s} \simeq \lambda, \tag{22}$$

and relates growth rate to the mass fraction of a 'bottleneck' transporter.

Combining Eqs. (19) and (22), we see that at steady-state the rate of import of the nutrient approximately matches its rate of metabolism:

$$\frac{\phi_m}{\tau_m} \frac{s_i}{K_m + s_i} \simeq \frac{\phi_t}{\tau_t} \frac{s}{K_t + s}. \tag{23}$$

#### S2.2.2 Determining ratios of enzymes

By solving the steady-state equations for $m_x$, $c_x$, and $e_x$, we find that

$$e_x = \frac{\frac{\gamma k_b \omega_x r}{\lambda n_x}}{(d_m + \lambda)\left(\frac{\gamma}{n_x} + k_u + \lambda\right) + \lambda k_b r} \tag{24}$$

and consequently that

$$\frac{e_m}{e_t} \simeq \frac{n_t \omega_m}{n_m \omega_t} \tag{25}$$

if either $n_m \simeq n_t$ or $\gamma / n_x \ll k_u + \lambda$ for both enzymes. More simply, the mass fractions are approximately given by the ratio of transcription rates

$$\frac{\phi_m}{\phi_t} \simeq \frac{\omega_m}{\omega_t}. \tag{26}$$

Further, if the dependencies of the two transcription rates on energy are approximately equal, then Eq. (26) implies that the ratio of mass fractions is approximately constant.

#### S2.2.3 Deriving the second law

Using Eqs. (19) and (22) in the equation for the conservation of mass

$$\phi_m + \phi_t + \phi_R = 1 - \phi_q, \tag{27}$$

we find

$$\phi_R \simeq 1 - \phi_q - \lambda \left[ \frac{K_m + s_i}{s_i} \cdot \tau_m + \frac{K_t + s}{s} \cdot \tau_t \right]. \tag{28}$$

From Eqs. (23) and (26),

$$\frac{\tau_m}{\tau_t} = \frac{\omega_m}{\omega_t} \cdot \frac{K_t + s}{s} \cdot \frac{s_i}{K_m + s_i} \tag{29}$$

and Eq. (28) then becomes

$$\phi_R \simeq 1 - \phi_q - \lambda \frac{K_t + s}{s} \cdot \tau_t \left[ \frac{\omega_m}{\omega_t} + 1 \right]. \tag{30}$$

Writing $\tau_e = \tau_t(1 + {}^{w_m}/_{w_t})$ to denote the enzyme synthesis time, which is the minimal time taken to import sufficient nutrient to synthesize both a transporter and a metabolic enzyme, then Eq. (30) becomes

$$\phi_R \simeq 1 - \phi_q - \lambda \frac{K_t + s}{s} \cdot \tau_e, \tag{31}$$

which is the second law. Note that empirically the second law holds when the extracellular media and so $s$ is constant. Again we have assumed that the rates of transcription of the two enzymes have a similar energy dependence so that ${}^{\omega_m}/_{\omega_t}$ is a constant. Note further that the enzyme synthesis time scales with the inverse of the nutrient efficiency, $\tau_e \sim 1/n_s$, explaining the slopes obtained in the translation inhibition experiments for varying nutrient conditions (Fig. 1B).

### S2.3 Monod's law

Using Eqs. (16), (19) and (22) in the conservation of mass equation, Eq. (27), gives

$$\lambda \left[ \frac{K_t + s}{s} \cdot \tau_e + \tau_\gamma \right] + \phi_r \simeq 1 - \phi_q, \tag{32}$$

or

$$\lambda \simeq \frac{1 - \phi_q - \phi_r}{\frac{K_t + s}{s} \tau_e + \tau_\gamma}. \tag{33}$$

Finally, if $\phi_r \ll \phi_q$ then

$$\lambda \simeq \frac{(1 - \phi_q) \cdot s}{K_t \tau_e + (\tau_e + \tau_\gamma) \cdot s}. \tag{34}$$

Changing the extracellular amount of nutrient can cause the ribosome synthesis time $\tau_\gamma$ to vary if levels of energy change. We conclude that Eq. (34) is Monod's law either

if the steady-state synthesis time $\tau_\gamma$ is approximately constant across different nutrient conditions (and so the translation elongation rate $\gamma$ is approximately constant) or if enzyme activity is growth-limiting so that

$$\frac{K_t + s}{s} \cdot \tau_e \gg \tau_\gamma. \tag{35}$$

Again note that the enzyme synthesis time $\tau_e$ depends on the inverse of the nutrient efficiency, and so for varying nutrient conditions Eq. (34) saturates with increasing nutrient efficiency $n_s$:

$$\lambda \simeq \frac{(1-\phi_q) s n_s}{(K_t + s)\frac{n_t}{v_t}\left(1 + \frac{\omega_m}{\omega_t}\right) + s\tau_\gamma n_s}, \tag{36}$$

where we have used the definitions of the synthesis times $\tau_e$ and $\tau_t$. To summarize, Monod growth follows from our model if either translational elongation is stable across different nutrient media (saturated, for example) or if enzyme activity is growth limiting.

Additional to the common relation between growth rate and nutrient abundance, the mechanistic derivation of Monod's law, Eq. (34), highlights the dependence on some experimentally accessible quantities: the nutrient, enzyme and ribosome efficiencies, and the load of house-keeping genes.

### S2.4 The impact of exogenous proteins on growth rate

If we cause the cell to express a protein $p$ that does not benefit the cell, then following the derivation of Eq. (33) we find that

$$\phi_p \simeq 1 - \phi_q - \phi_r - \lambda\left[\frac{K_t + s}{s} \cdot \tau_e + \tau_\gamma\right]. \tag{37}$$

If $\phi_r \ll \phi_q$ and if translation is growth-limiting, that is,

$$\frac{K_t + s}{s} \cdot \tau_e \ll \tau_\gamma, \tag{38}$$

then

$$\phi_p \simeq 1 - \phi_q - \tau_\gamma \lambda \tag{39}$$

or

$$\lambda \simeq \frac{1}{\tau_\gamma}(1 - \phi_q - \phi_p) \tag{40}$$

in analogy to the first law, Eq. (16), and in agreement with data from [18].

## S3 Parameter optimization, sensitivity and sloppiness

### S3.1 Including translational inhibition

To fit the data from [18], we considered a mechanism in which chloramphenicol, $c_m$, binds the mRNA-ribosome complexes, forming a 'zombie'-complex $\overline{zm}_x$, which is no

longer available to translation. We assume that the chloramphenicol concentration in the cell remains constant, i.e. $c_m$ is not consumed. Altogether, for each protein-type $x \in \{r, t, m, q\}$, we add a binding and a dilution reaction:

$$\begin{aligned} c_x &\xrightarrow{c_m \cdot k_{\mathrm{cm}}} \overline{zm}_x, \\ \overline{zm}_x &\xrightarrow{\lambda} \varnothing. \end{aligned} \tag{41}$$

The rate constant $k_{\mathrm{cm}}$ includes the conversion from the concentrations applied in [18] to molecule numbers and was fit as described below. To account for the extra reactions (41), we include equations for the chloramphenicol complexes and modify the equations of mRNA-ribosome complexes:

$$\dot{\overline{zm}}_x = c_x \cdot c_m k_{\mathrm{cm}} - \lambda \cdot \overline{zm}_x, \tag{42}$$

$$\dot{c}_x = -\lambda \cdot c_x + k_b \cdot r \cdot m_x - k_u \cdot c_x - \nu_x(c_x, a) \quad - \quad c_x \cdot c_m k_{\mathrm{cm}} \tag{43}$$

for $x \in \{r, t, m, q\}$ and with blue marking the modification to the original equations (6).

### S3.2 Parameter optimization

We fit the growth rate and the ribosomal mass fractions to data with translational inhibition (strain EQ2, columns 1 & 2 of Table S2 in [18]). We use the experimental chloramphenicol concentrations, $c_m \in \{0, 2, 4, 8, 12\}$ $\mu$M and model the different nutrient conditions by varying the nutrient efficiency, choosing $n_s$ as six equally log-spaced points between $n_s = 0.08$ and $n_s = 0.5$.

The parameters included in the estimation were the maximal transcription rates $w_x$, $x \in \{r, e, q\}$, the transcriptional energy-thresholds $\theta_r$ and $\theta_{\mathrm{nr}}$, the translational energy-threshold, $K_\gamma$ (through fitting $K_p = \gamma_{\max}/K_\gamma$), the auto-inhibition threshold $K_q$, and the chloramphenicol binding rate constant $k_{\mathrm{cm}}$. We estimated the eight parameters in a Bayesian fashion, using an adaptive Monte Carlo Markov chain method [11] to sample the posterior probability distribution for the parameters. The final estimates given in Table S2 are the modes of the resulting marginal posterior distributions.

### S3.3 Sensitivity and sloppiness

From the posterior distribution, we estimated the Fisher information matrix (FIM) by the pseudo-inverse of the variance-covariance matrix [15]. The eigenvalues of the FIM spread over orders of magnitude (Fig. S2A), indicating that the model is 'sloppy' [4, 10] and the parameters are not fine-tuned. Indeed, computing the parameter sensitivities from the FIM [15], we find that most parameters have low sensitivities (Fig. S2B). An exception is the maximal enzyme transcription rate, $w_e$, showing high sensitivity, because fixing the nutrient efficiencies, $n_s$, for the different experiments constrains $w_e$.

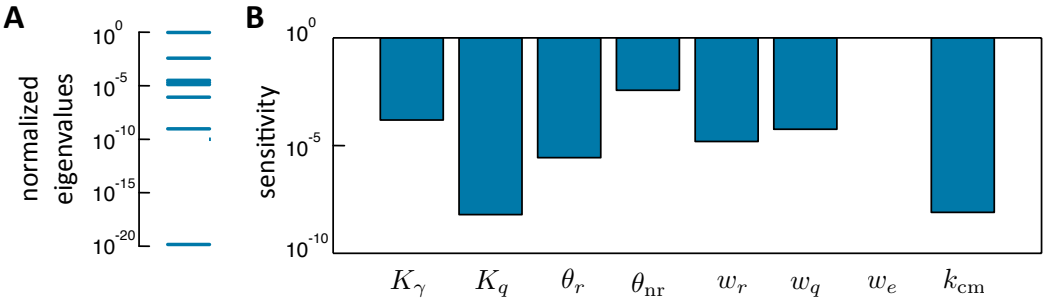


Figure S2: Fisher information. A The eigenvalues of the Fisher information matrix, normalized by the largest eigenvalue, spread over several orders of magnitude. B Parameter sensitivity with values close to one indicate that the model fit is sensitive to changes in the parameter.

# S4 Dosage compensation

## S4.1 Modelling paralog deletion

To model the deletion of a duplicate of the gene for an enzyme, we halve the maximal enzyme transcription rate in the deletion strain compared to the wild-type transcription rate: $w_e^{\Delta_e} = {}^{w_e}/_2$.

To model the expression of a gratuitous protein, denoted $p$, we included three new species, the protein itself and its free and ribosome-bound mRNA forms, $m_p$ and $c_p$, introducing equations, equivalent to Eqs. (4)–(6), for each:

$$\dot{p} = \nu_p(c_p, a) - \lambda \cdot p, \tag{44}$$

$$\dot{m}_p = \omega_p(a) - (\lambda + d_m) \cdot m_p + \nu_p(c_p, a) - k_b \cdot r \cdot m_p + k_u \cdot c_p, \tag{45}$$

$$\dot{c}_p = -\lambda \cdot c_p + k_b \cdot r \cdot m_p - k_u \cdot c_p - \nu_x(c_p, a). \tag{46}$$

We include the additional consumption of energy and ribosomes by

$$\begin{aligned} \dot{a} &= n_s \cdot \nu_{\mathrm{cat}}(e_m, s_i) - \lambda \cdot a - \sum_{\substack{x \in \\ \{r,t,m,q\}}} n_x \nu_x(c_x, a) \quad -n_p \nu_p(c_p, a), \\ \dot{r} &= \nu_r(c_r, a) - \lambda \cdot r + \sum_{\substack{x \in \\ \{r,t,m,q\}}} (\nu_x(c_x, a) - k_b \cdot r \cdot m_x + k_u \cdot c_x) \\ &\quad +(\nu_p(c_p, a) - k_b \cdot r \cdot m_p + k_u \cdot c_p), \end{aligned} \tag{47}$$

where blue marks the changes to the original Eqs. (2) & (3). Further, we modify the growth rate, (14) to include $p$-synthesis:

$$\lambda = \frac{\gamma(a)}{M} \left( \sum_{\substack{x \in \\ \{r,t,ms,q\}}} c_x + c_p \right). \tag{48}$$

We chose the maximal wild-type transcription rate equal to the transcription rate of the enzymes, $w_p = w_e$, and set $w_p^{\Delta_p} = w_p/2$ for the $\Delta_p$-strain. To see responsiveness of the same order of magnitude as in the $\Delta_e$-strain, we had to set maximal wild-type transcription for $p$-protein to ten times that of the enzymes, $w_p = 10w_e$ (not shown).

### S4.2 Responsiveness

We computed the responsiveness comparing the steady-state protein levels $x$ of the deletion, $\Delta_y$, $y \in \{e, p\}$, and the wild-type strains by [6]

$$R(x) = \log_2\left(\frac{x^{\Delta_y}}{\delta(x,y)\cdot x^{\mathrm{wt}}}\right), \qquad \delta(x,y) := \begin{cases} 1, & x \neq y \\ 0.5, & x = y \end{cases}, \tag{49}$$

where $\delta(x, y)$ ensures that we compare the expression of the remaining duplicate gene in the deletion strain with the expression of only one of the duplicate genes in the wild-type strain.

For each strain we compute the relative transcription rate of mRNA of type $x$ by

$$P(x) = \frac{\omega_x(a)}{\sum_y \omega_y(a)}, \tag{50}$$

as a measure of its ability to compete for ribosomes. We compare the relative transcription rates in the deletion strains $P_{\Delta_x}(\mathrm{nr})$, $x \in \{e, p\}$ with those in the wild-type strains $P_{\mathrm{wt}}(nr)$ in Fig. 2d.

## S5 Synthetic gene circuit

### S5.1 A host-aware model of the repressilator

We adapted the repressilator model from [9]. The repressilator-host model contains nine additional species compared to the original cell model: three mRNAs ($m_{g1}$, $m_{g2}$ and $m_{g3}$), their three ribosomal complexes ($c_{g1}$, $c_{g2}$ and $c_{g3}$), and the three proteins ($g_1$, $g_2$ and $g_3$). Theses species are involved in the reactions of Table S3 and give rise

Table S3: List of additional reactions in the repressilator-chassis model.

| | dilution/degr. | transcription | dilution/degradation | ribosome binding | translation |
|---|---|---|---|---|---|
| repressor 1 | $g_1 \xrightarrow{\lambda+d_g} \varnothing$ | $\varnothing \xrightarrow{\omega_{g1}} m_{g1}$ | $m_{g1} \xrightarrow{\lambda+d_{m,g}} \varnothing$ | $r + m_{g1} \underset{k_b}{\overset{k_u}{\longleftrightarrow}} c_{g1}$ | $n_g\, a + c_{g1} \xrightarrow{\nu_{g1}} r + m_{g1} + g_1$ |
| repressor 2 | $g_2 \xrightarrow{\lambda+d_g} \varnothing$ | $\varnothing \xrightarrow{\omega_{g2}} m_{g2}$ | $m_{g2} \xrightarrow{\lambda+d_{m,g}} \varnothing$ | $r + m_{g2} \underset{k_b}{\overset{k_u}{\longleftrightarrow}} c_{g2}$ | $n_g\, a + c_{g2} \xrightarrow{\nu_{g2}} r + m_{g2} + g_2$ |
| repressor 3 | $g_3 \xrightarrow{\lambda+d_g} \varnothing$ | $\varnothing \xrightarrow{\omega_{g3}} m_{g3}$ | $m_{g3} \xrightarrow{\lambda+d_{m,g}} \varnothing$ | $r + m_{g3} \underset{k_b}{\overset{k_u}{\longleftrightarrow}} c_{g3}$ | $n_g\, a + c_{g3} \xrightarrow{\nu_{g3}} r + m_{g3} + g_3$ |

to the differential equations:

$$\begin{aligned}
\dot{g}_i &= \nu_{gi}(c_{gi}, a) - (\lambda + d_g) \cdot g_i, \\
\dot{m}_{gi} &= \omega_{gi}(g_{i-1}, a) - (\lambda + d_{m,g}) \cdot m_{gi} + \nu_{gi}(c_{gi}, a) - k_b \cdot r \cdot m_{gi} + k_u \cdot c_{gi}, \\
\dot{c}_{gi} &= -\lambda \cdot c_{gi} + k_b \cdot r \cdot m_{gi} - k_u \cdot c_{gi} - \nu_{gi}(c_{go}, a), \qquad i = \{1, 2, 3\}\,.,
\end{aligned} \tag{51}$$

with $g_0 = g_3$. The transcription rates are defined by

$$\omega_{gi}(g_j, a) = w_g \cdot \frac{a}{\theta_{\mathrm{nr}} + a} \cdot R(g_j), \qquad R(g) := \frac{1}{1 + (g/K_g)^h}, \tag{52}$$

where $R(g)$ denotes the gene regulation function. The translation rates are defined analogously to (8) by

$$\nu_{gi}(c_{gi}, a) = c_{gi} \cdot \frac{\gamma(a)}{n_g}, \qquad i = \{1, 2, 3\}\,. \tag{53}$$

We include the additional consumption of energy and free ribosomes with:

$$\dot{a} = n_s \cdot \nu_{\mathrm{cat}}(e_m, s_i) - \lambda \cdot a - \sum_{\substack{x \in \\ \{r,t,m,q\}}} n_x \nu_x(c_x, a) \; - \sum_{i=\{1,2,3\}} n_g \nu_{gi}(c_{gi}, a),$$

$$\begin{aligned}
\dot{r} = \nu_r(c_r, a) - \lambda \cdot r + \sum_{\substack{x \in \\ \{r,t,m,q\}}} (\nu_x(c_x, a) - k_b \cdot r \cdot m_x + k_u \cdot c_x) \\
+ \sum_{i=\{1,2,3\}} (\nu_{gi}(c_{gi}, a) - k_b \cdot r \cdot m_{gi} + k_u \cdot c_{gi}).
\end{aligned} \tag{54}$$

Finally, following S1 the growth rate becomes:

$$\lambda = \frac{\gamma(a)}{M} \left( \sum_{\substack{x \in \\ \{r,t,m,q\}}} c_x + \sum_{i=\{1,2,3\}} c_{gi} \right). \tag{55}$$

with the value of $M$ unchanged.

**Parameters:** Transcript and protein half-lives were assumed to be two and four minutes, respectively [9], so that $d_{m,g} = {}^{\ln 2}/_{2}$ and $d_g = {}^{\ln 2}/_{4}$. The transcriptional parameters are: $K_g = 100$, $h = 2$ and $n_g = 300$ (equal to the length of the non-ribosomal proteins in Table S2). The induction level of the synthetic circuit, $w_g$, was varied in all simulations.

### S5.2 The isolated repressilator

We compared our host-aware repressilator with the standard model of an isolated repressilator [9]:

$$\dot{m}_{gi} = w_g \cdot R(g_{i-1}) - (d_{m,g} + \lambda_{\text{eff}}) \cdot m_{gi}, \qquad g_0 = g_3, \tag{56}$$

$$\dot{g}_i = k_{\text{eff}} \cdot m_{gi} - (d_g + \lambda_{\text{eff}}) \cdot g_i, \qquad i = \{1, 2, 3\}, \tag{57}$$

We used the same parameter values as the host-aware model. Additionally, we set the effective dilution rate, $\lambda_{\text{eff}} = 0.022$ min$^{-1}$, equal to the growth rate of the wild-type cell (without the synthetic circuit) for a nutrient efficiency of $n_s = 0.5$. We chose the effective translation rate, $k_{\text{eff}} = 0.6$ min$^{-1}$, so that the amplitudes of levels of repressors covered similar values as those in the host-aware model, at least for realistic value of $w_g < 10^3$mRNAs/ min, and varied induction within $w_g \in [1,\ 10^4]$.

### S5.3 The isolated model ignores resource trade-offs

The host-aware and the isolated models show qualitatively different behaviours (Fig. 3c, main text), but less so in rich nutrient conditions (Fig. S3). While the repressilator proteins oscillate substantially, the other cellular components maintain relatively stable levels (Fig. S4). We conclude that the differences between the behaviours of the two models are because the isolated model ignores depletion of resources within the host cell.

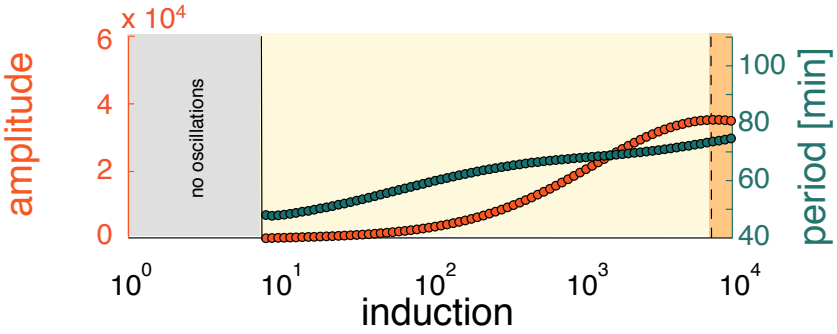


Figure S3: In rich conditions, the oscillations of the host-aware repressilator resemble those of the isolated repressilator (Fig. 3d, lower panel). Here, we used a high nutrient efficiency, $n_s = 15$ (cf. Fig. 3d in the main text with $n_s = 0.5$). As for the isolated repressilator, both period and amplitude grow with increasing induction. Only for unrealistically high induction ($w_g > 70\,000$ mRNAs/min), is the host over-loaded and the amplitude starts falling.

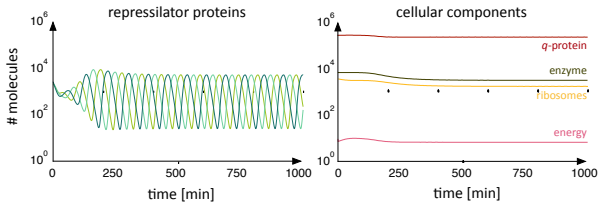


Figure S4: Oscillations in the repressilator proteins (left) barely affect the steady-state levels of other cellular components, which maintain stable levels (right). Here, $n_s = 0.5$, $s = 10\,000$ and the induction strength is $w_g = 614$ mRNAs/min), at which the amplitude of the oscillations is maximal (Fig. 3d).

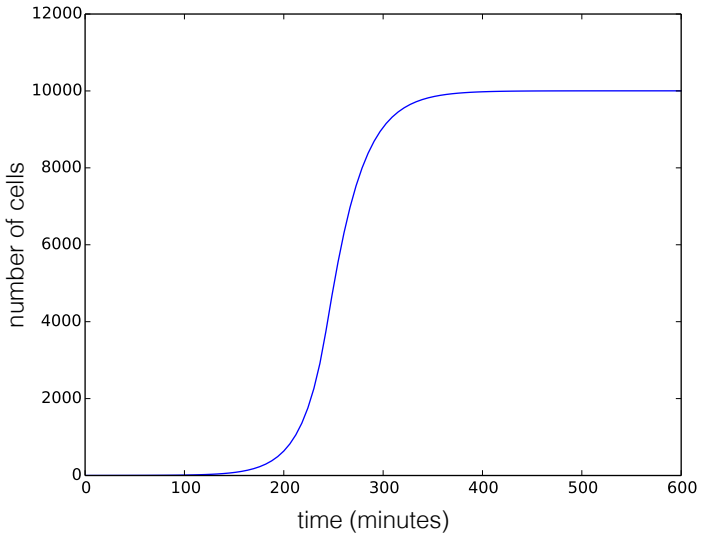


Figure S5: The multi-level model has a typical growth curve. We show the growth of a population of cells simulated using Eqs. (58) and (60) and the equations of Sec. S1 for all intracellular variables (although this example has an inducible metabolic pathway: see Sec. S6.2.1). Here we first simulated the intracellular reactions to steady-state with a fixed amount of extracellular nutrient to find suitable initial conditions. We then set the number of nutrient transporters to 1 (to give a lag) and simulated with an initial amount of $10^{10}$ nutrient molecules, which were not replenished. The population stopped growing shortly after extracellular nutrient was exhausted. Here $n_s = 100$ and $K_\gamma = 3.0 \times 10^8$.

# S6 Multiscale simulations and population growth

## S6.1 Including population growth

The growth of a homogenous population of cells can be straightforwardly included in our model. Assuming a death rate of individual cells of $d_N$, the total number of cells obeys

$$\dot{N} = \lambda N - d_N N \tag{58}$$

and grows exponentially if $\lambda > d_N$. For an intracellular molecule $x$, the total amount of $x$ in the population, $X = xN$, obeys

$$\dot{X} = \lambda X - d_N X + \dot{x} N \tag{59}$$

using the chain rule. If the rate of change of intracellular molecules is zero, $\dot{x} = 0$, then the population is in exponential growth because all quantities at the population level grow exponentially, providing $\lambda > d_N$.

To include the potential for competition between cells, we allow the external nutrient to change with time:

$$\dot{s} = k_{\text{in}} - \nu_{\text{imp}}(e_t, s) \cdot N - d_s s \tag{60}$$

with $k_{\text{in}}$ being a constant rate of influx and $d_s$ being a constant rate of efflux. To model growth in a chemostat, we would set $d_s = d_N$ with both equal to the chemostat's rate

of dilution. All other quantities, all of which are intracellular, obey the equations given in Sec. S1. Fig. S5 shows a typical growth curve.

If there is an influx of nutrient, the system goes to a steady-state with $\lambda = d_N$ from Eq. (58). The equation governing the total amount of energy either free or bound up in proteins, Eq. (20), becomes

$$\frac{d}{dt}\left[N(M + n_s s_i + a) + n_s s\right] = n_s(k_{\rm in} - d_s s) - d_N N(M + n_s s_i + a) \tag{61}$$

for a population of cells. At steady-state, then

$$N = \frac{n_s(k_{\rm in} - d_s s)}{d_N(M + n_s s_i + a)} \simeq \frac{n_s k_{\rm in}}{d_N M} \tag{62}$$

assuming $M \gg n_s s_i + a$ and $k_{\rm in} \gg d_s s$ under steady-state conditions.

## S6.2 Evolving gene regulation

### S6.2.1 Inducible gene expression

To investigate the evolution of gene regulation, we first extend the model to include inducible gene expression through a constitutively expressed transcription factor that, upon binding the nutrient, can activate expression of both a nutrient transporter and a metabolic enzyme. If $f$ and $b$ are the rates of binding and unbinding the nutrient, the transcription factor, $y$, satisfies

$$\begin{aligned} \dot{y} &= \nu_y(c_y, a) - \lambda y - f y s_i + b y_*, \\ \dot{y_*} &= f y s_i - b y_* - \lambda y_*, \end{aligned} \tag{63}$$

with $\nu_y$ given by Eq. (9) and $y_*$ denoting the activated transcription factor, a complex between $s_i$ and $y$. The transcription factor's mRNA obeys Eqs. (5) and (6) with $\omega_y$ satisfying Eq. (10). Finally, the rates of transcription of both the transporter and the metabolic enzyme are sigmoidal functions of $y_*$:

$$\omega_x(y_*, a) = \left[u + \frac{w_x y_*^h}{K_e^h + y_*^h}\right]\left[\frac{a}{\theta_x + a}\right], \tag{64}$$

with $K_e$ being the half-maximal, or threshold, amount of $y_*$ and $h$ being the Hill number. The constant $u$ gives a basal rate of transcription in the absence of $y_*$. As levels of nutrient rise so, too, do levels of activated transcription factor, and Eq. (64) ensures that expression of the nutrient transporter and of the metabolic enyzme correspondingly increase.

### S6.2.2 Invasion analysis

Our goal is to study gene regulation by determining the evolutionarily stable value of the threshold $K_e$ in Eq. (64). To compete a resident strain and a mutant, we first find the steady-state conditions of the resident. We simulate a single cell in an

environment with a fixed amount of nutrient to determine initial conditions and then simulate the growth to steady-state of a population of cells starting from one cell with these initial conditions but now in an environment with a constant influx of nutrients. To determine if a mutant can outcompete the resident, we augment the system with differential equations describing the growth of the mutant population. The mutants have initial conditions identical to the steady-state conditions of the resident except for the mutated value of the trait ($K_e$) and an initial number of mutants $10^6$ times smaller than the steady-state number of residents. The mutant and resident compete for the extracellular nutrient, and only the equation for the nutrient is affected by this competition:

$$\dot{s} = k_{\text{in}} - \nu_{\text{imp}}(e_t^{(r)}, s) \cdot N^{(r)} - \nu_{\text{imp}}(e_t^{(m)}, s) \cdot N^{(m)} - d_N s, \tag{65}$$

where superscripts indicate which population the variable belongs to and the population sizes have equations according to Eq. (58):

$$\dot{N}^{(r)} = \lambda^{(r)} N^{(r)} - d_N N^{(r)}, \tag{66}$$

$$\dot{N}^{(r)} = \lambda^{(m)} N^{(m)} - d_N N^{(m)}. \tag{67}$$

When the augmented system has reached steady-state, we score the outcome of the competition as $N_m/N_r+N_m$, which is one if the mutant invades completely and zero if the mutant goes extinct.

#### S6.2.3 Parameter values

Most parameter values are unchanged from Table S2 except $n_s = 100$ and $K_\gamma = 3.0 \times 10^8$. We set $d_s = d_N = 0.01$ min$^{-1}$ in Eq. (58); $f = 0.01$ min$^{-1}$ and $b = 1.4$ min$^{-1}$ in Eq. (63); $h = 2$ and $u = 3 \times 10^{-5}$ min$^{-1}$ in Eq. (64); and a maximum rate of transcription of the transcription factor of $w_y = 0.1$ min$^{-1}$.

#### S6.2.4 One extracellular nutrient

For a system with a single nutrient, the activation threshold $K_e$ evolves to maximize expression of the nutrient transporters (Fig. S6). A resident strain that always has more transporters than any possible mutant cannot be outcompeted.

#### S6.2.5 Two extracellular nutrients

To see more interesting evolution, we consider a system that can potentially metabolize two types of nutrient: $s_a$ and $s_b$. The genome has a transporter and a metabolic enzyme for each nutrient, and expression of both these genes is identically regulated and controlled by a constitutively expressed transcription factor, following Eq. (64). We fix $K_b$, the threshold for activation of the genes for nutrient $s_b$, but let $K_a$, the threshold for activation of the genes for $s_a$, evolve. Both nutrient systems have the same number of transcription factors and the same parameters except that the $b$ nutrient is energetically richer than then $a$ nutrient, $n_{s,b} = 100 n_{s,a}$, and that the $a$ genes are

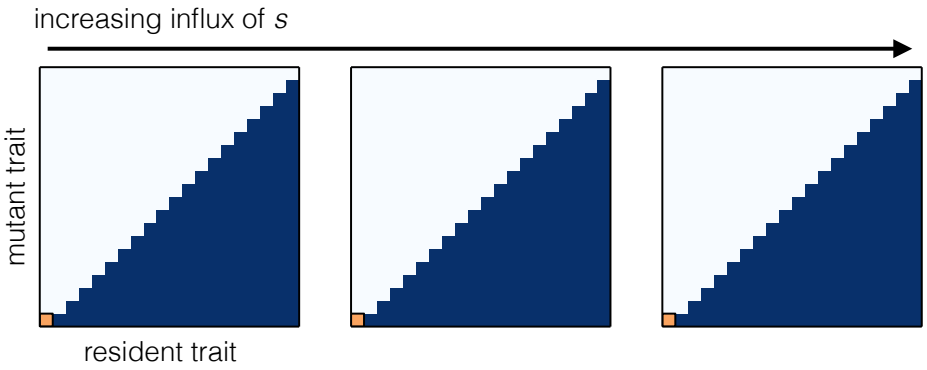


Figure S6: In an environment with a single nutrient, maximum and so constitutive expression of the nutrient transporter and enzyme is favoured. We show from left to right the invasion diagrams for $k_{\text{in}} \simeq 785\ \text{min}^{-1}$, $61,600\ \text{min}^{-1}$ and $127,000,000\ \text{min}^{-1}$. Mutants invade in blue regions and go extinct in white regions. For all influx rates, the evolutionary stable state (marked with an orange square) corresponds to the minimum dissociation constant $K_e$. DNA binding of the activated transcription factor is therefore maximized and so is gene expression.

more strongly expressed, $w_a = 10w_b$. Each extracellular nutrient obeys an equation similar to Eq. (65), and we implemented the invasion analysis analogously to the single nutrient example (Sec. S6.2.2).

We can also derive an expression equivalent to Eq. (62). The total energy of the system is

$$N\left[M + \sum_k n_{s,k}\left(s_{i,k} + y_{*,k}\right) + a\right] + \sum_k n_{s,k} s_k, \tag{68}$$

where the sum is over all nutrients and recalling that $y_*$ is a complex of $y$ and a nutrient $s_i$. Differentiating the total energy with respect to time and setting the result to zero (and imposing $\lambda = d_N$ from Eq. (58)), we find that

$$N = \frac{\sum_k n_{s,k}\left(k_{\text{in},k} - d_N s_k\right)}{d_N\left[M + \sum_k n_{s,k}\left(s_{i,k} + y_{*,k}\right) + a\right]} \tag{69}$$

at steady-state.

## Supplementary References

[1] K. R. Albe, M. H. Butler, and B. E. Wright. Cellular concentrations of enzymes and their substrates. *Journal of theoretical biology*, 143(2):163–195, 1990.

[2] F. Brandt, S. A. Etchells, J. O. Ortiz, A. H. Elcock, F. U. Hartl, and W. Baumeister. The native 3d organization of bacterial polysomes. *Cell*, 136(2):261–271, 2009.

[3] H. Bremer and P. Dennis. Modulation of chemical composition and other parameters of the cell by growth rate. In C. Neidhardt, editor, Escherichia coli *and* Salmonella. ASM Press, Washington, DC, 1996.

[4] K. S. Brown and J. P. Sethna. Statistical mechanical approaches to models with many poorly known parameters. *Physical Review E*, 68(2):021904, 2003.

[5] W. Cleland. Partition analysis and concept of net rate constants as tools in enzyme kinetics. *Biochemistry*, 14(14):3220–3224, 1975.

[6] A. DeLuna, M. Springer, M. W. Kirschner, and R. Kishony. Need-based up-regulation of protein levels in response to deletion of their duplicate genes. *PLoS Biol*, 8(3):e1000347, 03 2010.

[7] K. Dornmair, P. Overath, and F. Jähnig. Fast measurement of galactoside transport by lactose permease. *Journal of Biological Chemistry*, 264(1):342–346, 1989.

[8] M. Ehrenberg and C. Kurland. Costs of accuracy determined by a maximal growth rate constraint. *Quarterly reviews of biophysics*, 17(01):45–82, 1984.

[9] M. B. Elowitz and S. Leibler. A synthetic oscillatory network of transcriptional regulators. *Nature*, 403(6767):335–338, 2000.

[10] R. N. Gutenkunst, J. J. Waterfall, F. P. Casey, K. S. Brown, C. R. Myers, and J. P. Sethna. Universally sloppy parameter sensitivities in systems biology models. *PLoS computational biology*, 3(10):e189, 2007.

[11] H. Haario, M. Laine, A. Mira, and E. Saksman. DRAM: efficient adaptive MCMC. *Statistics and Computing*, 16(4):339–354, 2006.

[12] I. M. Keseler, J. Collado-Vides, A. Santos-Zavaleta, M. Peralta-Gil, S. Gama-Castro, L. Muñiz Rascado, C. Bonavides-Martinez, S. Paley, M. Krummenacker, T. Altman, P. Kaipa, A. Spaulding, J. Pacheco, M. Latendresse, C. Fulcher, M. Sarker, A. G. Shearer, A. Mackie, I. Paulsen, R. P. Gunsalus, and P. D. Karp. Ecocyc: a comprehensive database of escherichia coli biology. *Nucleic Acids Research*, 39(suppl 1):D583–D590, 2011.

[13] S. Klumpp, M. Scott, S. Pedersen, and T. Hwa. Molecular crowding limits translation and cell growth. *Proceedings of the National Academy of Sciences*, 110(42):16754–16759, 2013.

[14] S. Klumpp, Z. Zhang, and T. Hwa. Growth rate-dependent global effects on gene expression in bacteria. *Cell*, 139(7):1366–1375, 2009.

[15] M. Komorowski, M. J. Costa, D. A. Rand, and M. P. Stumpf. Sensitivity, robustness, and identifiability in stochastic chemical kinetics models. *Proceedings of the National Academy of Sciences*, 108(21):8645–8650, 2011.

[16] J. Monod. The Growth of Bacterial Cultures. *Annual review of microbiology*, 3(1):371–394, Oct. 1949.

[17] J. B. Russell and G. M. Cook. Energetics of bacterial growth: balance of anabolic and catabolic reactions. *Microbiological reviews*, 59(1):48–62, 1995.

[18] M. Scott, C. W. Gunderson, E. M. Mateescu, Z. Zhang, and T. Hwa. Interdependence of cell growth and gene expression: origins and consequences. *Science (New York, NY)*, 330(6007):1099–1102, Nov. 2010.

[19] M. Scott and T. Hwa. Bacterial growth laws and their applications. *Current opinion in biotechnology*, 22(4):559–565, Aug. 2011.

[20] Y. Taniguchi, P. J. Choi, G.-W. Li, H. Chen, M. Babu, J. Hearn, A. Emili, and X. S. Xie. Quantifying e. coli proteome and transcriptome with single-molecule sensitivity in single cells. *Science*, 329(5991):533–538, 2010.

[21] A. Wagner. Energy constraints on the evolution of gene expression. *Molecular biology and evolution*, 22(6):1365–1374, 2005.

[22] J. R. Warner. The economics of ribosome biosynthesis in yeast. *Trends in biochemical sciences*, 24(11):437–440, 1999.